Linear microstability investigation of a Neon impurity seeded FTU plasma

C.Mazzotta[1], V.Dolci[2], M. Marinucci[1], G. Pucella[1], M.E.Puiatti[3], M.Romanelli[4], G. Szepesi[4], O. Tudisco[1] and the FTU team*

[1]*ENEA, Dipartimento FSN, C. R. Frascati, via E. Fermi 45, 00044 Frascati (Roma), Italy*

[2]*Dip. SBAI, "Sapienza" Università di Roma, Via Antonio Scarpa 14/16, 00161 Roma, Italy*

[3]*Consorzio RFX, Corso Stati Uniti 4, 35127 Padova, Italy*

[4]*Culham Centre for Fusion Energy, OX14 3DB, Abingdon, UK*

**See the appendix of G. Pucella et al., proceedings of the 25th IAEA Fusion Energy Conference, Saint Petersburg, Russia, 2014*

The effect of impurity seeding comes back to collect a deep renewed interest, due to its large use to dissipate energy and to preserve the divertor in fusion devices. As a matter of fact, this method is expected to be used in future reactors. Moreover, this modus operandi can generate the positive side effect of plasma detachment. In this context the effect of seeding have to be further investigated in particular by deepening related transport mechanisms that often affect the whole plasma column from the edge to the core.

In FTU ohmic plasmas the seeding of Neon impurity (in the absence of Deuterium gas puffing) causes a rise of line averaged electron density up to a factor two, associated with a significant increase of the peaking factor [1].

As for the particle transport and the microturbolence analysis, the mechanism of density peaking can be linked to the growth rates of Ion and Electron Temperature Gradients modes (ITG, ETG). This is the motivation of a detailed linear micro-stability analysis presented in this paper. It has been carried out with the gyrokinetic code GKW on a Neon injected discharge in terms of presence of modes, growth rates and fluxes of species.

Experiment and data used for the gyrokinetic analysis

The effects of Neon seeding have been studied in a series of dedicated ohmic discharge. Some important observations have been collected, the principal regarding the spontaneous increase of the line averaged density up to a factor two; furthermore, a dependence has been found on the amount of the impurity injected and plasma current [1].

Two similar discharges were produced in the same experimental session: one with a Neon injection at 0.6 s for 50 msec and a second one at the same current and toroidal field, but with exclusively Deuterium gas, reaching the same line-average electron density, to be used as reference undoped pulse. As a consequence of the injection, the doped pulse get colder in the outer region up to half radius. The behavior of the two discharges is shown in figure 1, both pulses were performed at the same central line density (upper frame: #37342 Neon injected pulse with red traces, #37344 reference pulse with blue traces); an impressive density peaking rise of Neon injected discharge in respect to the undoped one was found (second panel); as well as the parallel increase of the radiation losses (third frame); finally the improved energy confinement in the central region is ameliorated (last frame). In order to better understand how the presence of the impurity affects the particle transport a stability analysis was performed with a gyrokinetic code.

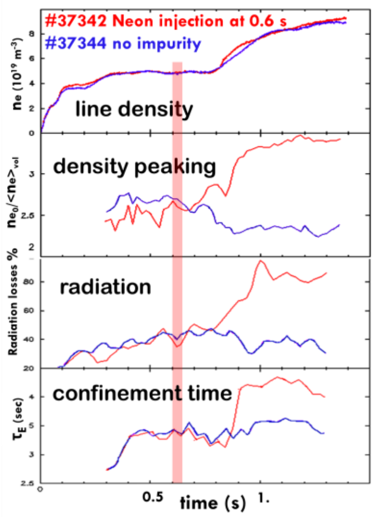

Figure 1. Time traces of some relevant quantities. The light red vertical box marks the Neon injection period.

The gyrokinetic analysis

Several simulations have been conducted using the fully electromagnetic Gyrokinetics@Warwick (GKW) code [2], that solves the self-consistent Vlasov–Maxwell equations, in the gyro-centre approximation. The local linear analysis is intended for qualitative comparison of the linear growth rates and particle fluxes. The eigenfunctions and fluxes calculated by the code are normalized every time step and they are associated with the dominant mode for a specific wave vector. The magnitude of the flux therefore does not carry information about the saturated flux level, but its sign indicates the direction of the flux in the linear phase of the mode growth. In this analysis the $\vec{E} \times \vec{B}$ contribution is taken into account and the gyro-centre flux is calculated by GKW neglecting terms of order ρ_*^2 [3,4,5].

In figure 2 the growth rates versus the perpendicular normalized wavenumber $k_\theta \rho_i$ of ETG and ITG are shown for both the

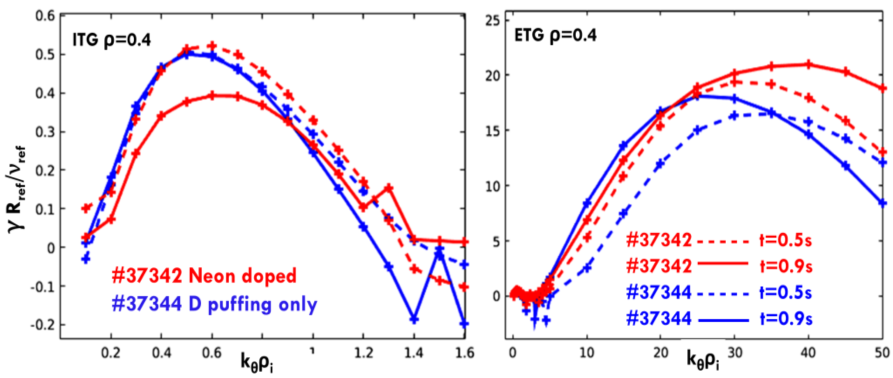

Figure 2. Scan in time of the growth rates (normalized at a reference major radius and reference ion temperature for this radius) as a function of the bi-normal wavenumber, at normalized radius ρ=0.4 for the doped (red traces) and the undoped pulse (blue lines). At left: the small wave number region where the ITG modes are dominan, at right: ETG whole spectra. The time of 0.5 s refers to the pre-injection (dotted line), while at 0.9 s the effects of the impurity are well established (continuous traces).

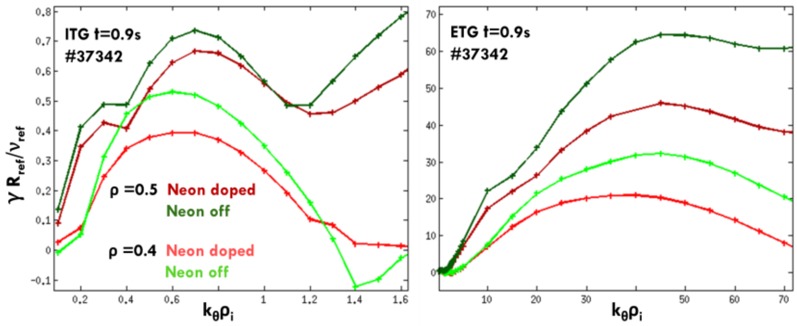

Figure 3. Scan in radius of the growth rates as a function of the bi-normal wavenumber at the time of 0.9 s for the doped discharge (red lines): at left panel ITG, at right the ETG modes. The green traces represent the same pulse with the Neon specie set to zero in the simulation. The intensity of the color indicates the radius: lighter for internal, darker for half radius.

discharges, at two different times: pre and post injection. For higher wavenumbers, with the peak around 40, the ETG is the dominant instability (right panel), whereas in the small wavenumber region (<2) the ITG modes dominate (left panel, positive values). The figure reproduces the growth rates at the normalized radius ρ = 0.4, but they exhibit a similar behavior even at different values of the radius. Before the density rise, the growth rates of the ITG modes appear almost coincident in both the discharges (dotted traces), whereas, at t=0.9 s only the Neon injected pulse presents lower ITG growth rates as a consequence of the enhanced steepness of the density profile (left frame, red continuous line).

In order to appreciate the direct effect of the Neon presence at fixed gradients, it's more appropriate to compare the doped discharge with itself where the impurity is suppressed.

This is exposed in figure 3: the green traces represent the GKW growth rates simulation of the #37342 pulse with the Neon specie concentration set to zero. The ITG modes (left frame), as well as the ETG (right frame) with the impurity (outlined by the red traces) are systematically lower than the green ones, to mean the stabilizing effect due to the direct presence of Neon on these modes.

In order to figure out how different Neon profiles affects the analysis, three different impurity configurations have been used as input in the GKW code. The first two simulations consist of different flat concentrations, whereas the third is a more realistic radial profile estimated by an Impurity Transport Code [6]. In figure 4 the ETG and ITG are reproduced for these different flat concentrations (light blue trace = 1% and blue trace =2%) and for a peaked shape (1%, red trace) as calculated in ref. [6]. In terms of ETG the stabilizing effect is due to the amount of Neon injected, while for the ITG the beneficial effect derives from the peaking shape of the impurity profile. For subsequent analyzes carried out in this work, the peaked 1% Neon profile has been used.

GKW can produce for each wavenumber $k_\theta\rho_i$ the radial structure of the modes, as scalar and vector potential, for the components: real and imaginary. The fluxes directions of the species are useful to identify the modes presence, knowing that the drift waves for ITG, ETG and

TEM (Trapped Electron Modes) have even parity for the scalar and odd for the parallel vector potential. The scalar potential is three order of magnitude higher than the vector potential, implying that the modes are essentially electrostatic. For the scalar potential the even parity is confirmed as well as the odd one for the vector potential. In these simulated conditions one can neglect the presence of Tearing and Microtearing modes.

Finally, the fluxes analysis shows that for the ETG case, that is relevant in building up the overall density profile, these modes drive the inward flux for electrons and Deuterium, if compared with the pre injection time. Different is the behavior of the Neon specie, indeed it is found to be outward at an internal radius (ρ=0.4), it becomes yet inward for a more external radius (ρ=0.6).

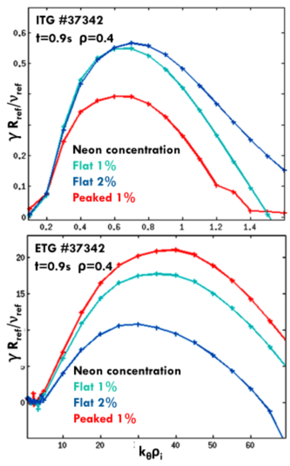

Figure 4. Effect on the Growth rates of the Neon concentration: blue for flat profiles (1%, 2%); red for peaked shape at 1%. Upper/lower panel for ITG/ETG respectively.

Conclusions

GKW code has been used to establish the role of the impurity in determining the growth rates of the unstable modes and driving the peaking of the electron density profiles. A stabilizing effect has been found as consequence of the Neon injection, which extends its effects up to the center. The shaping of the Neon impurity reconstructed profile, used as input in the simulations, plays an important role in determining the evolution on the modes.

The radial structure of the modes suggests the prevalence of electrostatics drift modes.

The fluxes analysis reveals that the sharp peaking of the density profile is mainly due to the inward pinch brought about by ETG modes.

"The computing resources and the related technical support used for this work have been provided by CRESCO/ENEAGRID High Performance Computing infrastructure and its staff. CRESCO/ENEAGRID High Performance Computing infrastructure is funded by ENEA, the Italian National Agency for New Technologies, Energy and Sustainable Economic Development and by Italian and European research programs, see http://www.cresco.enea.it/english for information".

[1] Mazzotta C. et al. 2015 Nucl. Fusion **55** 073027 (7pp)

[2] Peeters A.G. et al. 2009 Comput. Phys. Commun. **180** 2650

[3] Murakami M. et al. 2001 Nucl. Fusion **41** 317

[4] Romanelli M. et al. 2011 Nucl. Fusion **51** 103008 (9pp)

[5] Szepesi G. et al. Nucl. Fusion **53** 033007

[6] Mazzotta C. et al. *Neon transport simulation for highly peaked dens*.. 42nd EPS Conf. on Pl. Phys., Lisbon, 22-26 June, 2015. Vol. 39E ISBN 2-914771-98-3. P4.114 http://ocs.ciemat.es/EPS2015PAP/pdf/P4.114.pdf